



Suppression of Obesity by an Intestinal Helminth through Interactions with Intestinal Microbiota

Chikako Shimokawa,^a Seiji Obi,^a Mioko Shibata,^a Alex Olia,^a Takashi Imai,^a Kazutomu Suzue,^a Hajime Hisaeda^b

^aDepartment of Parasitology, Graduate School of Medicine, Gunma University, Gunma, Japan

^bDepartment of Parasitology, National Institute of Infectious Diseases, Tokyo, Japan

ABSTRACT Obesity is increasingly causing lifestyle diseases in developed countries where helminthic infections are rarely seen. Here, we investigated whether an intestinal nematode, *Heligmosomoides polygyrus*, has a suppressive role in diet-induced obesity in mice. Infection with *H. polygyrus* suppressed weight gain in obese mice, which was associated with increased uncoupling protein 1 (UCP1) expression in adipocytes and a higher serum norepinephrine (NE) concentration. Blocking interactions of NE with its receptor on adipocytes resulted in the failure to prevent weight gain and to enhance UCP1 expression in obese mice infected with *H. polygyrus*, indicating that NE is responsible for the protective effects of *H. polygyrus* on obesity. In addition to sympathetic nerve-derived NE, the intestinal microbiota was involved in the increase in NE. Infection with *H. polygyrus* altered the composition of intestinal bacteria, and antibiotic treatment to reduce intestinal bacteria reversed the higher NE concentration, UCP1 expression, and prevention of the weight gain observed after *H. polygyrus* infection. Our data indicate that *H. polygyrus* exerts suppressive roles on obesity through modulation of microbiota that produce NE.

KEYWORDS helminth, immunity, obesity, microbiota

Obesity causes lifestyle diseases such as hypertension, diabetes, and dyslipidemia (1). Excess energy consumption is an important cause of obesity. The overall body energy balance is maintained by adjusting excess or deficient energy in conjunction with energy intake and output. One such metabolic control is present in adipose tissues. Adipose tissue is classified as white or brown (2), with each having different characteristics. White adipose tissue accumulates excessive lipids as triglycerides, while brown adipose tissue consumes fatty acids as heat (3). Brown adipose tissues contain two distinct types of thermogenic adipocytes: classical brown adipocytes and beige or bright adipocytes. A major goal of research on obesity is to understand the factors that activate thermogenic adipocytes, which activate energy consumption, thus preventing obesity.

Uncoupling protein 1 (UCP1) is an integral membrane protein expressed in the mitochondria of brown (4) and beige (5) adipocytes, and it uncouples oxidative phosphorylation. When UCP1 is activated, energy generated by the lipolysis of fatty acids and glucose is directly converted to heat, without being directed to ATP synthesis, and the heat then dissipates (6). Thus, this molecule is crucial for energy expenditure. Heat production by UCP1 is controlled by norepinephrine (NE), which is released from sympathetic nerves that are densely distributed in brown fat. Fatty acids are generated through lipolysis that is induced by NE acting on its receptor and driving activation of adipocyte lipases, including adipose triglyceride lipase and hormone-sensitive lipase. The fatty acid produced is oxidatively decomposed and activates UCP1. When NE acts on white adipocytes, fat decomposition similarly occurs, but the fatty acid produced is released into the blood and is consumed by brown

Citation Shimokawa C, Obi S, Shibata M, Olia A, Imai T, Suzue K, Hisaeda H. 2019. Suppression of obesity by an intestinal helminth through interactions with intestinal microbiota. *Infect Immun* 87:e00042-19. <https://doi.org/10.1128/IAI.00042-19>.

Editor DeBroski R. Herbert, University of Pennsylvania

Copyright © 2019 Shimokawa et al. This is an open-access article distributed under the terms of the [Creative Commons Attribution 4.0 International license](https://creativecommons.org/licenses/by/4.0/).

Address correspondence to Hajime Hisaeda, hisa@niid.go.jp.

Received 17 January 2019

Returned for modification 20 February 2019

Accepted 16 March 2019

Accepted manuscript posted online 8 April 2019

Published 21 May 2019

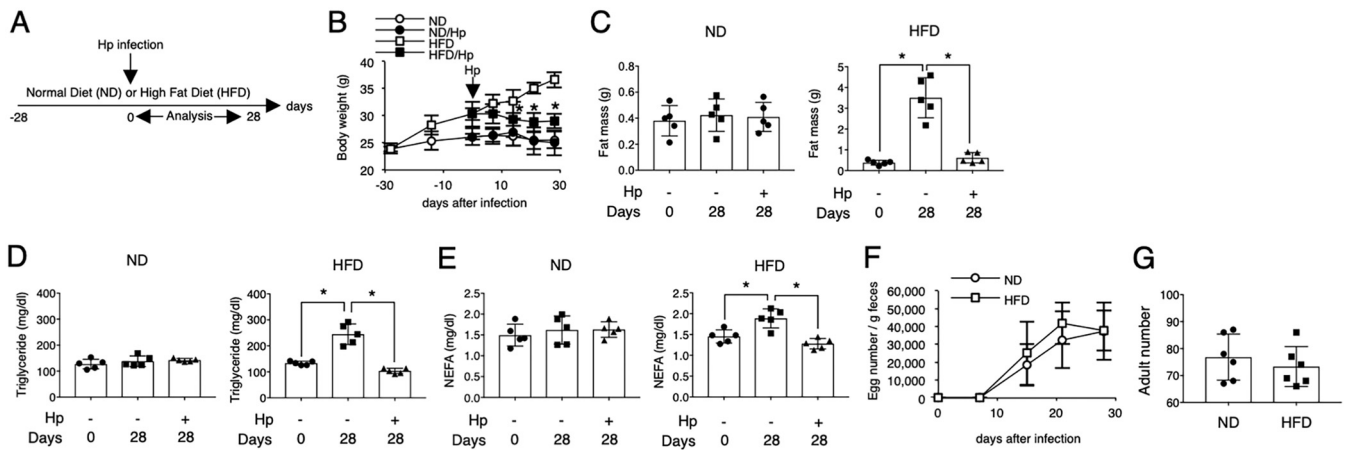


FIG 1 Reduction of preexisting obesity in mice infected with *Heligmosomoides polygyrus* (Hp). (A) Experimental protocol for generating obese mice. Mice fed a high-fat diet (HFD) for 28 days were orally infected with 200 L3 *H. polygyrus* larvae, and the HFD was continued for the entire experimental period. A normal diet (ND) was used as a control. All analyses were performed 28 days after infection unless otherwise mentioned. (B) Body weight of mice fed an HFD or an ND in the presence or absence of *H. polygyrus* infection was periodically monitored. The weight of epididymal adipose tissue (C) and the blood concentration of triglycerides (D) and nonesterified fatty acid (NEFA) (E) in the indicated groups were measured. (F and G) The number of *H. polygyrus* eggs per gram of feces was monitored weekly, and the number of adult worms in the small intestine was counted 28 days after infection in mice fed an HFD or an ND. All values are presented as the means \pm standard deviations of five or six mice in one representative experiment. Symbols in scatter graphs with bars represent data from an individual animal. Similar results were obtained from three replicate experiments. *, $P < 0.05$, by Student's *t* test or two-way ANOVA.

adipocytes and muscle. A characteristic of beige adipocytes is the dynamic regulation of UCP1 by external stimuli. β 3-Adrenergic receptor (β 3AdR) agonists induced the marked expression of UCP1 in beige adipocytes (5).

Recent studies demonstrated a close relationship between intestinal microbiota composition and several diseases, including metabolic, gastrointestinal, and inflammatory diseases (7, 8). Additionally, obesity is associated with low gut microbiota diversity, and it may alter the composition of certain bacteria in humans and animal models (9). Many factors that affect the onset of obesity are associated with modulation of the microbiota (10, 11). The intestinal microbiota is associated with psychiatric diseases including depression and autism, and previous studies reported that intestinal bacteria communicated with the central nervous system to stimulate the production of neurotransmitters and hormones, including serotonin, dopamine, and γ -amino butyric acid (12–14).

The incidence of obesity has increased, especially in developed countries where helminthic infections have almost been eliminated (15). Several lines of evidence indicate an inverse correlation between helminthic infections and obesity as well as inflammation-mediated disorders (16, 17), suggesting that helminths may have suppressive effects on these diseases. However, protective mechanisms involved in how helminths suppress obesity are largely unknown. Given that intestinal helminths modulate gut microbiota, the current study investigated the effects of an intestinal nematode on obesity in mice fed a high-fat diet (HFD) by focusing on the gut microbiota. We found that helminthic infection affected gut bacteria, resulting in increased NE production that upregulated UCP1 in adipose tissues.

RESULTS

Infection with *Heligmosomoides polygyrus* reduces established obesity. To investigate whether infection with *Heligmosomoides polygyrus* has therapeutic effects on established obesity, we used mice fed an HFD for 4 weeks as infection hosts (Fig. 1A). This diet resulted in an increase in body weight up to 20% and an increase in fat mass and dyslipidemia (Fig. 1B to E), and these mice were considered obese. Before analysis, we confirmed that feeding with an HFD had no adverse effect on *H. polygyrus* infection. Obese mice harbored adult worms and produced eggs at levels comparable to those of mice fed a normal diet (ND) (Fig. 1F and G). Continuously feeding obese mice an HFD

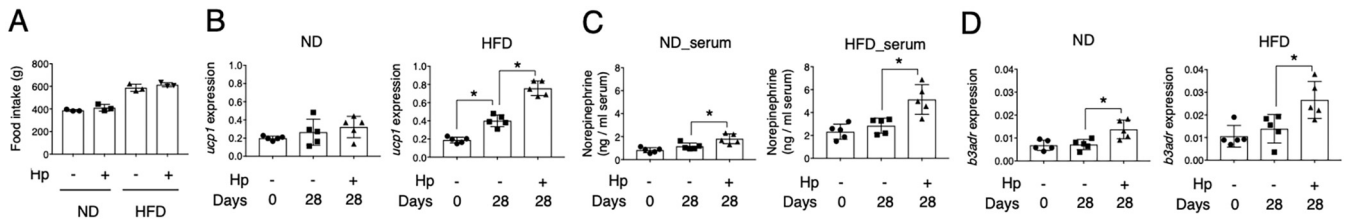


FIG 2 Potential causes of obesity correction during *H. polygyrus* infection. (A) The amount of food intake by each group was measured. Consumption of the diet by each group comprised of five mice housed in one cage was estimated by subtracting the weight of food remaining after 1 week of feeding from the original weight of the food provided, and this measurement was repeated for 4 weeks. Values represent the means \pm standard deviations of three individual experiments. (B) mRNA encoding UCP1 in adipocytes obtained from epididymal adipose tissues of the indicated groups. The expression level relative to GAPDH mRNA is presented. (C) The NE concentration in the blood obtained from the indicated group was determined by ELISA. (D) mRNA encoding β 3AdR was quantified as described for panel B. All values in panels B, C, and D are presented as the means \pm standard deviations of five mice in one representative experiment. Symbols in scatter graphs with bars represent data from an individual animal. Similar results were obtained from three replicate experiments. *, $P < 0.05$, using a two-way ANOVA.

accelerated the increase in body weight. Infection of obese mice with *H. polygyrus* decreased body weight and improved dyslipidemia (Fig. 1B to E). These results suggested that *H. polygyrus* infection has preventive and therapeutic effects on existing obesity.

***H. polygyrus*-mediated reduction in obesity is associated with UCP1 expression induced via NE.** Because food intake in obese mice was not influenced by infection with *H. polygyrus* (Fig. 2A), weight loss might be a result of excess calorie consumption rather than of a reduction of calorie intake. We postulated that, in addition to a marked decrease in fat mass (Fig. 1C), *H. polygyrus* infection might promote energy generation in adipose tissues, which is controlled by UCP1 expression in adipocyte mitochondria. Thus, UCP1 mRNA expression in adipocytes obtained from *H. polygyrus*-infected obese mice was quantified (Fig. 2B). Although UCP1 was substantially upregulated even in the absence of *H. polygyrus* as obesity proceeded, infection with *H. polygyrus* induced significantly more UCP1 expression. UCP1 expression in adipocytes is regulated by sympathetic innervation through the production of NE (18). In parallel with UCP1 expression, obese mice infected with *H. polygyrus* showed the highest concentration of NE in the blood (Fig. 2C). Released NE acts on β 3AdR expressed on white adipocytes. We also analyzed the mRNA expression of β 3AdR in adipocytes, and the same trends as for UCP1 and NE were observed: obesity increased β 3AdR expression, and infection with *H. polygyrus* had additional effects (Fig. 2D). Infection of nonobese ND-fed mice with *H. polygyrus* resulted in a slight increase in NE levels and the expression of β 3AdR, but it had no effect on UCP1 expression (Fig. 2B to D). These results suggest that UCP1 expression is dependent on NE- β 3AdR interactions, which may be responsible for the reduction of obesity in obese mice infected with *H. polygyrus*. To test this possibility, a selective antagonist of β 3AdR, SR59230 (19), was administered to *H. polygyrus*-infected obese mice. Blockade of β 3AdR did not alter the ability to produce eggs in either obese or nonobese mice (Fig. 3A). Mice treated with SR59230 failed to suppress weight gain even in the presence of *H. polygyrus* (Fig. 3B). Although SR59230 did not affect the NE concentration, it markedly suppressed the increased UCP1 mRNA expression (Fig. 3C and D). In mice fed an ND, there was no change in body weight, NE concentration, or UCP1 expression (Fig. 3B to D). Thus, the protective role of *H. polygyrus* infection against obesity is dependent on NE, presumably by inducing UCP1 for energy expenditure in adipocytes.

Neurogenic NE contributes to the *H. polygyrus*-mediated reduction of obesity.

We next analyzed the mechanisms involved in the production of NE during *H. polygyrus* infection. Infection of obese mice with *H. polygyrus* resulted in an increase in NE concentrations in the serum and adipose tissues (Fig. 4A). Because sympathetic innervation is the major source of NE in adipose tissues (20), *H. polygyrus*-infected obese mice were subjected to chemical denervation by treatment with reserpine. This agent blocks the intake of catecholamine into presynaptic vesicles and therefore allows

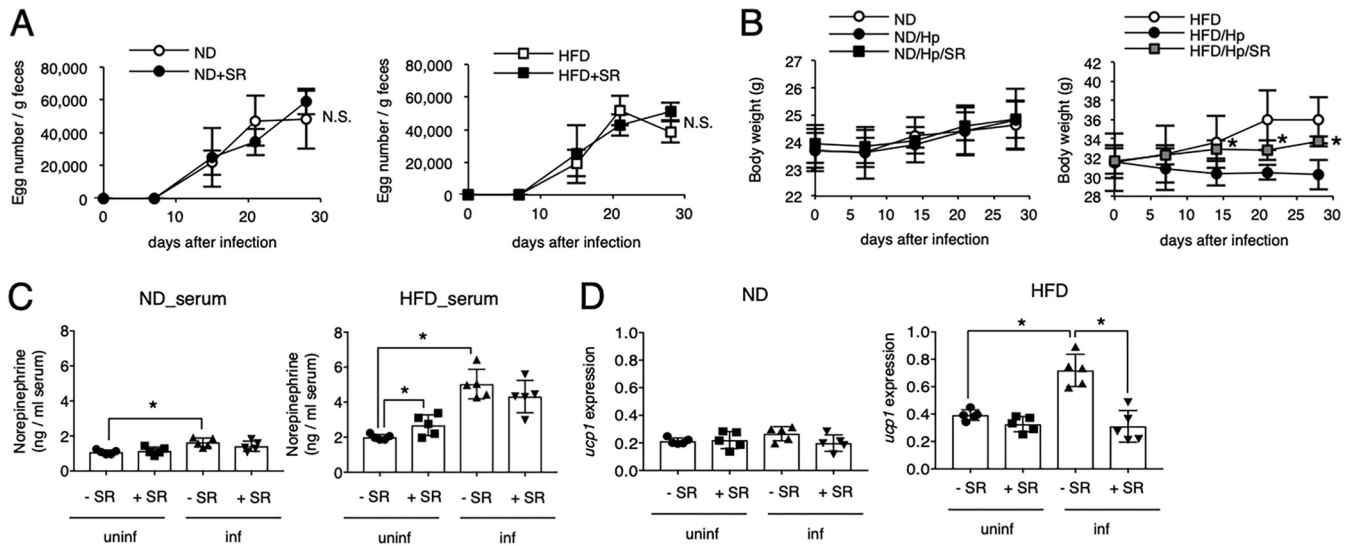


FIG 3 Critical roles of NE in the anti-adiposity effects of *H. polygyrus* infection. (A) The number of *H. polygyrus* eggs per gram of feces in mice treated with a β 3AdR antagonist, SR59230A (SR), was monitored weekly. (B) Body weight of obese mice infected with *H. polygyrus* in the presence of SR was monitored. (C and D) The serum NE concentration and UCP1 mRNA expression level in the indicated mouse group were evaluated as described in the legend of Fig. 2. All values are presented as the means \pm standard deviations of five mice in one representative experiment. Symbols in scatter graphs with bars represent data from an individual animal. *, $P < 0.05$; N.S., not significant (using a two-way ANOVA). uninfect, uninfected; inf, infected.

assessment of nervous system involvement in the suppression of obesity. Mice treated with reserpine produced similar numbers of eggs as untreated mice (Fig. 4B). In the absence of infection, treatment with reserpine significantly reduced the NE concentration and expression of UCP1 in adipose tissue, resulting in increased body weight in mice fed with an ND and an HFD (Fig. 4A, C, and D). Similarly, *H. polygyrus*-infected mice treated with reserpine exhibited lower NE concentrations and lower expression levels of UCP1 (Fig. 4A and C). Suppression of obesity observed in *H. polygyrus*-infected obese mice was attenuated in the presence of reserpine (Fig. 4D), indicating the involvement of neurogenic NE in the expression of UCP1 and the suppression of weight gain.

The intestinal microbiota is involved in the *H. polygyrus*-mediated reduction of obesity. Although treatment of uninfected mice with reserpine completely suppressed NE production in adipose tissues and serum, obese mice infected with *H. polygyrus* still contained substantial amounts of NE after treatment with reserpine (Fig. 4A), suggesting the existence of other sources of NE besides sympathetic nerves. Thus, we next addressed how *H. polygyrus* induces NE production by focusing on the intestinal microbiota (i) because *H. polygyrus* parasitizes small intestines and affects the microbiota (16, 17) and (ii) because several neurotransmitters, including NE, originate from the microbiota (21, 22). In addition, infection of obese mice with *H. polygyrus* increased NE levels in the feces (Fig. 5A). To this end, obese mice infected with *H. polygyrus* were orally treated with antibiotics to reduce the intestinal microbiota (Fig. 5B). This treatment did not affect the parasitism of *H. polygyrus* as assessed by egg production (Fig. 5C). Treatment with antibiotics decreased both the NE concentration and expression of UCP1 in *H. polygyrus*-infected obese mice, resulting in the attenuated suppression of weight gain (Fig. 5D to G). Thus, the microbiota has a crucial role in the *H. polygyrus*-mediated prevention of obesity.

Infection with *H. polygyrus* changes the intestinal microbiota in obese mice. To investigate changes in the microbiota responsible for the increase in NE production during infection with *H. polygyrus*, the fecal microbiota of *H. polygyrus*-infected mice was comprehensively analyzed. Feeding with the HFD alone altered the composition of microbiota, characterized by a decrease in *Proteobacteria* and an increase in unassigned bacteria (Fig. 6A). Mice infected with *H. polygyrus* contained more representatives of the *Firmicutes* and *Proteobacteria* than uninfected mice independent of diet they were fed

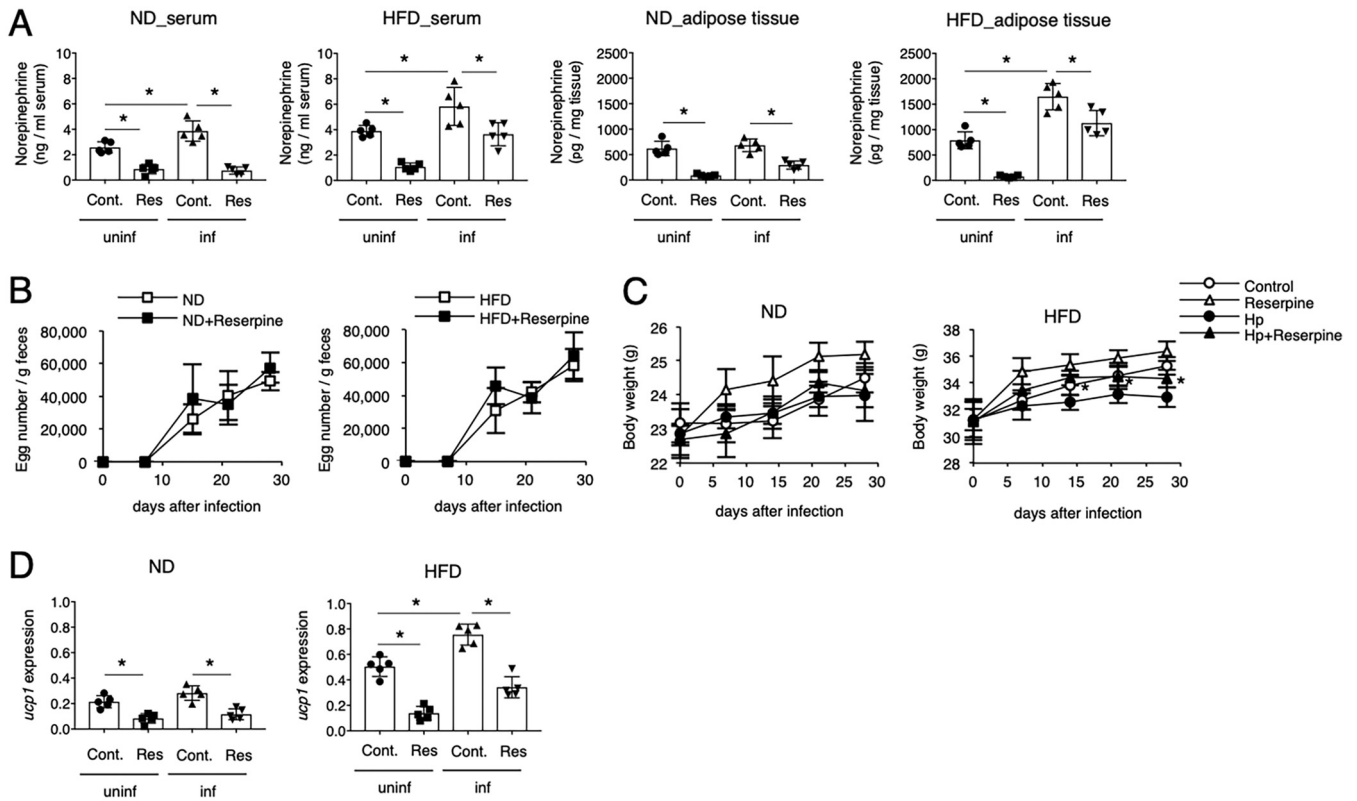


FIG 4 Involvement of neurogenic NE in the *H. polygyrus*-mediated suppression of weight gain. Serum and adipose tissue NE concentrations (A), the number of *H. polygyrus* eggs per gram of feces (B), body weight (C), and UCP1 mRNA expression (D) in mice treated with reserpine (Res) were monitored. All values are presented as the means \pm standard deviations of five mice in one representative experiment. Symbols in scatter graphs with bars represent data from an individual animal. Cont, control. *, $P < 0.05$, using a two-way ANOVA.

(Fig. 6A and B). Previous studies reported that two bacterial genera, *Bacillus* and *Escherichia* belonging to *Firmicutes* and *Proteobacteria*, respectively, produced NE in the intestines (23). Quantitative real-time PCR analyses of microbiota revealed that infection of obese mice with *H. polygyrus* significantly increased *Bacillus* and *Escherichia* species (Fig. 6C). In addition, the NE concentration in *H. polygyrus*-infected obese mice was closely correlated with the amounts of those bacteria (Fig. 6D). These results suggest that infection with *H. polygyrus* modulates intestinal bacteria to produce NE, which is responsible for limiting weight gain.

DISCUSSION

In this study, we demonstrated that *H. polygyrus* suppressed HFD-induced obesity. Mechanistically, *H. polygyrus* affected the composition of the intestinal microbiota to increase NE, resulting in enhanced UCP1 expression in adipose tissues. Because stimulation with NE was reported to induce beige adipocytes from adipocyte progenitors associated with UCP1 expression (5), these thermogenic adipocytes might be induced during *H. polygyrus* infection.

Recently, Su et al. reported the preventive effects of *H. polygyrus* infection on HFD-induced obesity, focusing on distinct immune responses (24). Alternative activated macrophages (AAMs) induced during *H. polygyrus* infection suppressed insulin resistance and inflammation associated with obesity and enhanced UCP1 expression in adipose tissues. We also think that the decisive effector that prevents obesity is increased UCP1 expression. However, we revealed different mechanisms from those of Su et al. involving AAMs that upregulated UCP1 expression. This difference may be due to difference in experimental system, and our system elicited mild obesity without causing hyperglycemia or insulin resistance. Although we did not investigate immune

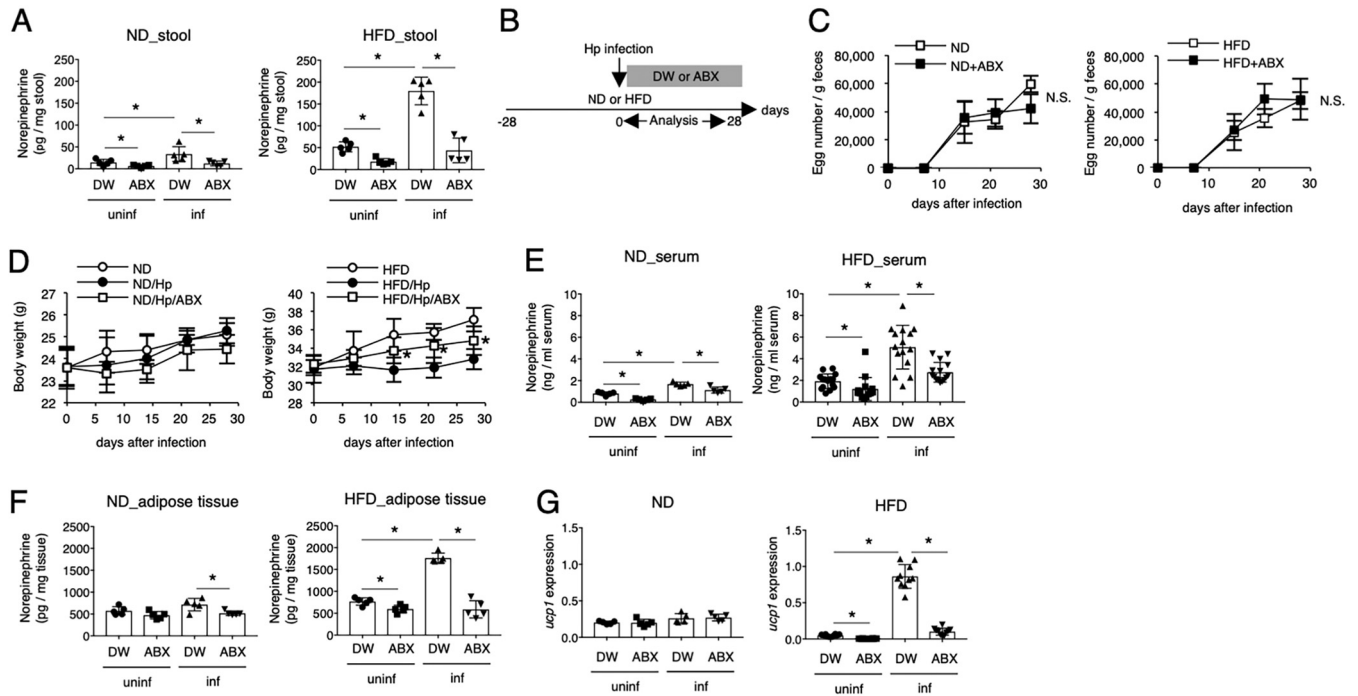


FIG 5 Involvement of intestinal microbiota in NE production in obese mice infected with *H. polygyrus*. (A) Fecal NE concentrations in the indicated mice were analyzed. (B) Scheme for the treatment of *H. polygyrus*-infected obese mice with antibiotics (ABX). The number of *H. polygyrus* eggs per gram of feces (C), body weight (D), NE concentration in serum (E) and adipose tissue (F), and UCP1 mRNA expression (G) in the indicated mouse groups were evaluated as described in the legends of Fig. 2 and 4. All values are presented as the means \pm standard deviations of more than five mice in one representative experiment. Symbols in scatter graphs with bars represent data from an individual animal. *, $P < 0.05$, using a two-way ANOVA. DW, distilled water.

responses, mild obesity was not associated with inflammation, indicating that it may be regulated in ways other than by immune responses.

Our results using a $\beta 3$ AdR antagonist demonstrated that NE plays a crucial role in UCP1 expression. Chemical denervation using reserpine increased body weight even in the absence of *H. polygyrus* infection, indicating that neurogenic NE primarily regulates the induction of UCP1 under physiological conditions. In addition to neurogenic NE,

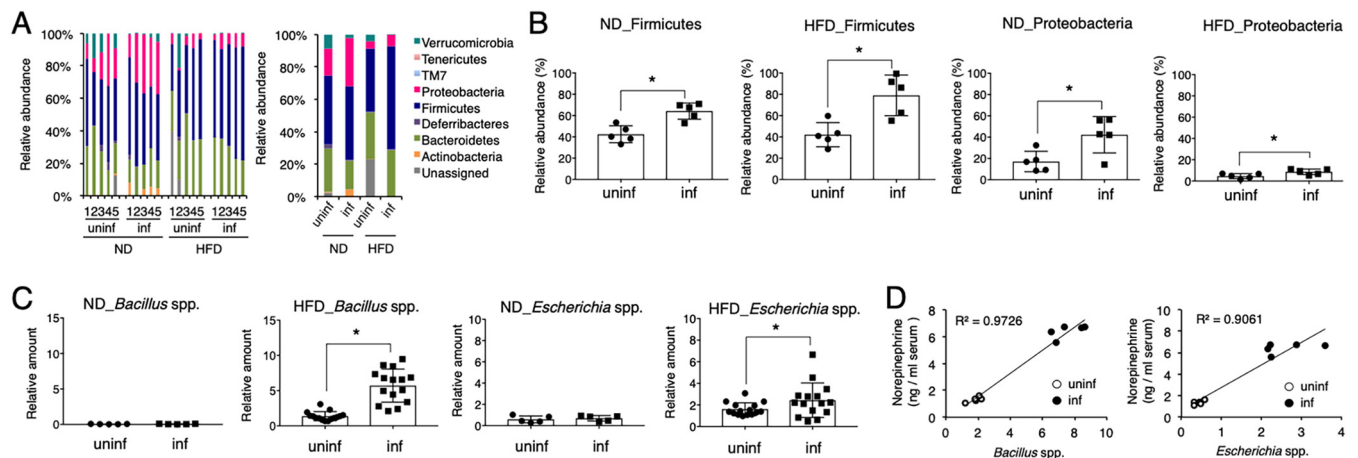


FIG 6 Changes in intestinal microbiota in obese mice infected with *H. polygyrus*. (A) Composition of intestinal microbiota at the phylum level in the indicated mouse groups is shown. Each bar in the left and right panels depicts the composition of an individual mouse and the mean value from five mice, respectively. (B) The frequency of *Firmicutes* and *Proteobacteria* in mice represented by the data in panel A is shown. (C) The abundances of *Bacillus* and *Escherichia* species in the overall intestinal microbiota in mice 28 days after infection were calculated based on quantitative PCR, as described below. Relative abundance (%) = $2^{(CT_{universal} 16S - CT_{specific} 16S)} \times 100$, where C_T is threshold cycle. All values are presented as the means \pm standard deviations of more than five mice in one representative experiment. *, $P < 0.05$, using a two-way ANOVA. (D) The representative coplotted NE concentration and abundance of genera in five individual mice in the presence or absence of *H. polygyrus* infection 28 days after infection are presented. R^2 , the correlation coefficient.

intestinal microbiota contributed to increased NE levels in obese mice infected with *H. polygyrus*. Because *H. polygyrus* resides in the small intestine, it is thought to affect the intestinal microbiota. Several studies demonstrated that the intestinal flora composition was altered after *H. polygyrus* infection (25, 26). Here, we observed that *H. polygyrus* infection altered the gut microbiota composition, and, specifically, more *Bacillus* and *Escherichia* species were detected, both of which are known to generate NE (14, 27). Other bacterial products such as short-chain fatty acids are known to have anti-obesity effects, and some bacteria are associated with obesity (28); therefore, additional effects caused by changes in microbiota may contribute to the reduction of obesity. Thus, comprehensive analyses of the intestinal microbiota are required to understand metabolic homeostasis better during *H. polygyrus* infection.

The question arises as to whether the induction of NE is favorable to *H. polygyrus* parasitism. The expulsion of intestinal worms depends on the production of mucin and peristaltic movements controlled by parasympathetic nerves. Thus, the activation of sympathetic nerves may help intestinal parasites to settle by suppressing intestinal movement. However, this seems unlikely because egg production was not decreased by treatment with the β 3AdR agonist or antibiotics (Fig. 3A and 5C). We did not address how *H. polygyrus* modulates the microbiota at the molecular level. Further analyses to determine which molecules are involved will be valuable to treat or prevent obesity, such as by using prebiotics and probiotics.

MATERIALS AND METHODS

Mice. Male C57BL/6J mice were purchased from Japan SLC (Hamamatsu, Japan), maintained under specific pathogen-free conditions, and used for experiments at 10 to 12 weeks of age. For experimental feeding, an HFD containing 60% fat (HFD-60; Oriental Yeast Corporation, Tokyo, Japan) and a control normal diet (AIN-93M; Oriental Yeast Corporation) were used. All animal experiments were reviewed and approved by the Committee for Ethics on Animal Experiments at the Graduate School of Gunma University (approval number 16-041) and were conducted under the control of the Guidelines for Animal Experiments in the Graduate School of Gunma University and in accordance with Law No. 105 and Notification No. 6 of the Japanese Government.

***H. polygyrus* infection.** Infectious stage III *H. polygyrus* larvae (L3) were prepared as previously described (29) and stored at 4°C until use. Mice were inoculated orally with 200 L3 larvae using gastric intubation. Eggs in feces were detected using a microscope to confirm successful infection.

Sample collection. Blood was taken from the mice via cardiac puncture under anesthesia, and mice were sacrificed by cervical dislocation. Epididymal adipose tissue was aseptically removed, and adipocytes were purified as previously reported (30). The adipose tissue weight was then measured. Serum samples were separated from the collected blood for analyses. In some experiments, all adult worms recovered from the small intestine of mice infected with *H. polygyrus* were counted.

Serum analysis. Serum samples were analyzed for triglyceride and nonesterified fatty acid (NEFA) using LabAssay (Wako, Tokyo, Japan) and for NE using a standard enzyme-linked immunosorbent assay (ELISA), in accordance with the manufacturer's instructions (ISM, Tokyo, Japan).

Real-time RT-PCR analysis. Total RNA was extracted from purified adipocytes using an RNeasy Mini kit (Qiagen, Hilden, Germany) and reverse transcribed using ReverTra Ace (Toyobo, Osaka, Japan) to synthesize cDNA. Resultant cDNA expressing the genes of interest was quantified, by real-time reverse transcription-PCR (RT-PCR) using SYBR green (TaKaRa Bio, Shiga, Japan), relative to the level of mRNA encoding glyceraldehyde-3-phosphate dehydrogenase (GAPDH) in accordance with the manufacturer's protocol. The specific primer pairs were as follows: for *Ucp1*, 5'-ACTGCCACACCTCCAGTCATT-3' and 5'-CTTTGCCTCACTCAGGATTGG-3'; for *Adrb3*, 5'-TCGACATGTCCTCCACCAA-3' and 5'-GATGGTCCAAGATGGTGCTT-3'; and for *Gapdh*, 5'-TGTGTCCGTCGTGGATCTGA-3' and 5'-TTGCTGTTGAAGTCGCAGGAG-3'.

Receptor blockade. For β 3 adrenergic receptor blockade, 5 mg/kg body weight of SR59230 (Sigma, St. Louis, MO, USA) was intraperitoneally injected every other day for 28 days (31).

Reserpine injection. Reserpine (0.5 mg/kg body weight) was intraperitoneally injected 1 day before and 3 and 5 days after *H. polygyrus* infection.

Antibiotic treatment. To reduce gut bacteria, obese mice infected with *H. polygyrus* were administered a mixture of ampicillin (1 g/liter), vancomycin (0.5 g/liter), neomycin (1 g/liter), and metronidazole (1 g/liter) in their drinking water for 28 days.

Gut microbiota analysis by 16S rRNA sequencing. Fecal samples collected from mice were immediately frozen in liquid nitrogen and stored at -80°C. Fecal DNA extraction was performed according a previous study with minor modifications (32). A grain of mouse feces was suspended with sterilized sticks in 475 μ l of TE10 buffer containing 10 mM Tris-HCl (pH 8.0) and 10 mM EDTA. The fecal suspension was incubated with 15 mg/ml lysozyme (Wako) at 37°C for 1 h. A final concentration of 2,000 units/ml of purified achromopeptidase (Wako) was added and then incubated at 37°C for 30 min. We added 1% (wt/vol) sodium dodecyl sulfate and 1 mg/ml proteinase K (Merck Japan, Tokyo, Japan) to the suspension and incubated it at 55°C for 1 h. After centrifugation of the suspension, bacterial DNA was purified using phenol-chloroform-isoamyl alcohol (25:24:1) solution. DNA was precipitated by adding

ethanol and sodium acetate. RNase A (Wako) was added to bacterial DNA in TE buffer to a final concentration 1 mg/ml. To remove fragmented low-molecular-weight DNA, precipitation with polyethylene glycol (PEG) 6000 was performed after RNase treatment.

The V4 variable region (residues 515F to 806R) was sequenced on an Illumina MiSeq, according to the method of Kozich et al. (33). Each reaction mixture contained 15 pmol of each primer, 0.2 mM deoxyribonucleoside triphosphates, 5 μ l of 10 \times Ex Taq HS buffer, 1.25 U Ex Taq HS polymerase (TaKaRa Bio), 50 ng of extracted DNA, and sterilized water to a final volume of 50 μ l. PCR conditions were as follows: 95°C for 2 min, 25 cycles of 95°C for 20 s, 55°C for 15 s, and 72°C for 5 min, followed by 72°C for 10 min. The PCR product was purified by AMPure XP (Beckman Coulter, Brea, CA, USA) and quantified using a Quant-iT PicoGreen double-stranded DNA (dsDNA) assay kit (Life Technologies Japan, Tokyo, Japan). Mixed samples were prepared by pooling approximately equal amounts of PCR amplicons from each sample. The pooled library was analyzed with an Agilent High Sensitivity DNA kit on an Agilent 2100 Bioanalyzer (Agilent Technologies, CA, USA). Real-time PCR for quantification was performed on a pooled library using a KAPA Library Quantification kit for Illumina according to the manufacturer's protocols. Based on the quantification, the sample library was denatured and diluted. A sample library with 20% denatured PhiX spike-in was sequenced by MiSeq using a 500-cycle kit. We obtained 2- by 250-bp paired-end reads. Taxonomic assignments and the estimation of relative abundances from sequencing data were performed using the analysis pipeline of the QIIME software package (34).

Quantification of fecal microbiota with real-time PCR. DNA from mouse stools was extracted using a Stool Mini kit (Qiagen). Genes encoding 16S rRNA were quantified using a reverse transcription-quantitative PCR (RT-qPCR) kit (Qiagen). The specific primer pairs were as follows: for *Escherichia* spp., 5'-GTTAATACCTTTGCTCATTGA-3' and 5'-ACCAGGGTATCTAATCCTGTT-3' (35); for *Bacillus* spp., 5'-CAGTAGGAATCTTCCGCAATG-3' and 5'-AGCCGTGGCTTTCTGGT-3' (36). A universal primer pair for all bacteria was also used: 5'-GTGGTGCACGGCTGTCTCA-3' and 5'-ACGTCATCCACCTTCTC-3' (37).

Statistical analysis. Group means were compared by two-way analysis of variance (ANOVA), followed by Tukey's *post hoc* test or two-tailed Student's *t* test. Probability values below 0.05 were considered statistically significant.

ACKNOWLEDGMENTS

We thank Wakana Mizutani for technical assistance and Jodi Smith from the Edanz Group (Fukuoka, Japan) for editing a draft of the manuscript.

This work was supported by a Grant-in-Aid for International Scientific Research (B) from the Japan Society for the Promotion of Science (15H05274 to H.H.), a Grant-in-Aid for Young Scientists (B) (26870849 to C.S.), and a Grant-in-Aid for Scientific Research (C) (15K08441 to H.H.) from the Ministry of Education, Culture, Sports, Science, and Technology; a grant was also provided by the Ichiro Kanehara Foundation Japan and Takeda Science Foundation.

REFERENCES

- Halpern A, Mancini MC, Magalhaes ME, Fisberg M, Radominski R, Bertolami MC, Bertolami A, de Melo ME, Zanella MT, Queiroz MS, Nery M. 2010. Metabolic syndrome, dyslipidemia, hypertension and type 2 diabetes in youth: from diagnosis to treatment. *Diabetol Metab Syndr* 2:55. <https://doi.org/10.1186/1758-5996-2-55>.
- Kajimura S. 2017. Adipose tissue in 2016: Advances in the understanding of adipose tissue biology. *Nat Rev Endocrinol* 13:69–70. <https://doi.org/10.1038/nrendo.2016.211>.
- Sanchez-Gurmaches J, Hung C-M, Guertin DA. 2016. Emerging complexities in adipocyte origins and identity. *Trends Cell Biol* 26:313–326. <https://doi.org/10.1016/j.tcb.2016.01.004>.
- Walker JE, Runswick MJ. 1993. The mitochondrial transport protein superfamily. *J Bioenerg Biomembr* 25:435–446. <https://doi.org/10.1007/BF01108401>.
- Kajimura S, Spiegelman BM, Seale P. 2015. Brown and beige fat/physiological roles beyond heat generation. *Cell Metab* 22:546–559. <https://doi.org/10.1016/j.cmet.2015.09.007>.
- Busiello RA, Savarese S, Lombardi A. 2015. Mitochondrial uncoupling proteins and energy metabolism. *Front Physiol* 6:36. <https://doi.org/10.3389/fphys.2015.00036>.
- Backhed F, Ley RE, Sonnenburg JL, Peterson DA, Gordon JI. 2005. Host-bacterial mutualism in the human intestine. *Science* 307:1915–1920. <https://doi.org/10.1126/science.1104816>.
- Neish AS. 2009. Microbes in gastrointestinal health and disease. *Gastroenterology* 136:65–80. <https://doi.org/10.1053/j.gastro.2008.10.080>.
- Wolf KJ, Lorenz RG. 2012. Gut microbiota and obesity. *Curr Obes Rep* 1:1–8. <https://doi.org/10.1007/s13679-011-0001-8>.
- Boothman OA, Zamzami MA, Taher I, Abubaker J, Abu-Farha M. 2016. The role of gut microbiota in the development of obesity and diabetes. *Lipids Health Dis* 15:108. <https://doi.org/10.1186/s12944-016-0278-4>.
- Diamant M, Blaak EE, de Vos WM. 2011. Do nutrient-gut-microbiota interactions play a role in human obesity, insulin resistance and type 2 diabetes? *Obes Rev* 12:272–281. <https://doi.org/10.1111/j.1467-789X.2010.00797.x>.
- Strandwitz P. 2018. Neurotransmitter modulation by the gut microbiota. *Brain Res* 1693:128–133. <https://doi.org/10.1016/j.brainres.2018.03.015>.
- Sarkar A, Lehto SM, Harty S, Dinan TG, Cryan JF, Burnet PWJ. 2016. Psychobiotics and the manipulation of bacteria-gut-brain signals. *Trends Neurosci* 39:763–781. <https://doi.org/10.1016/j.tins.2016.09.002>.
- Dinan TG, Stilling RM, Stanton C, Cryan JF. 2015. Collective unconscious: how gut microbes shape human behavior. *J Psychiatr Res* 63:1–9. <https://doi.org/10.1016/j.jpsychires.2015.02.021>.
- Bhurosy T, Jeewon R. 2014. Overweight and obesity epidemic in developing countries: a problem with diet, physical activity, or socioeconomic status? *ScientificWorldJournal* 2014:964236. <https://doi.org/10.1155/2014/964236>.
- Weinstock JV, Elliott DE. 2014. Helminth infections decrease host susceptibility to immune-mediated diseases. *J Immunol* 193:3239–3247. <https://doi.org/10.4049/jimmunol.1400927>.
- Wang LJ, Cao Y, Shi HN. 2008. Helminth infections and intestinal inflammation. *World J Gastroenterol* 14:5125–5132. <https://doi.org/10.3748/wjg.14.5125>.
- Inokuma K, Ogura-Okamoto Y, Toda C, Kimura K, Yamashita H, Saito M. 2005. Uncoupling protein 1 is necessary for norepinephrine-induced

- glucose utilization in brown adipose tissue. *Diabetes* 54:1385–1391. <https://doi.org/10.2337/diabetes.54.5.1385>.
19. Galitzky J, Langin D, Verwaerde P, Montastruc JL, Lafontan M, Berlan M. 1997. Lipolytic effects of conventional beta 3-adrenoceptor agonists and of CGP 12,177 in rat and human fat cells: preliminary pharmacological evidence for a putative beta 4-adrenoceptor. *Br J Pharmacol* 122: 1244–1250. <https://doi.org/10.1038/sj.bjp.0701523>.
 20. Bartness Lab J, Langin D, Verwaerde P, Montastruc JL, Lafontan M, Berlan M. 2014. Neural innervation of white adipose tissue and the control of lipolysis. *Front Neuroendocrinol* 35:473–493. <https://doi.org/10.1016/j.yfrne.2014.04.001>.
 21. Holzer P, Farzi A. 2014. Neuropeptides and the microbiota-gut-brain axis. *Adv Exp Med Biol* 817:195–219. https://doi.org/10.1007/978-1-4939-0897-4_9.
 22. Galland L. 2014. The gut microbiome and the brain. *J Med Food* 17: 1261–1272. <https://doi.org/10.1089/jmf.2014.7000>.
 23. Mazzoli R, Pessione E. 2016. The neuro-endocrinological role of microbial glutamate and GABA signaling. *Front Microbiol* 7:1934. <https://doi.org/10.3389/fmicb.2016.01934>.
 24. Su CW, Chen CY, Li Y, Long SR, Massey W, Kumar DV, Walker WA, Shi HN. 2018. Helminth infection protects against high fat diet-induced obesity via induction of alternatively activated macrophages. *Sci Rep* 8:4607. <https://doi.org/10.1038/s41598-018-22920-7>.
 25. Zaiss MM, Rapin A, Lebon L, Dubey LK, Mosconi I, Sarter K, Piersigilli A, Menin L, Walker AW, Rougemont J, Paerewijck O, Geldhof P, McCoy KD, Macpherson AJ, Croese J, Giacomini PR, Loukas A, Junt T, Marsland BJ, Harris NL. 2015. The intestinal microbiota contributes to the ability of helminths to modulate allergic inflammation. *Immunity* 43:998–1010. <https://doi.org/10.1016/j.immuni.2015.09.012>.
 26. Walk ST, Blum AM, Ewing SA, Weinstock JV, Young VB. 2010. Alteration of the murine gut microbiota during infection with the parasitic helminth *Heligmosomoides polygyrus*. *Inflamm Bowel Dis* 16:1841–1849. <https://doi.org/10.1002/ibd.21299>.
 27. Cryan JF, Dinan TG. 2012. Mind-altering microorganisms: the impact of the gut microbiota on brain and behaviour. *Nat Rev Neurosci* 13: 701–712. <https://doi.org/10.1038/nrn3346>.
 28. Chandra KC. 2015. New-found link between microbiota and obesity. *World J Gastrointest Pathophysiol* 6:110–119. <https://doi.org/10.4291/wjgp.v6.i4.110>.
 29. Shimokawa C, Kanaya T, Hachisuka M, Ishiwata K, Hisaeda H, Kurashima Y, Kiyono H, Yoshimoto T, Kaisho T, Ohno H. 2017. Mast cells are crucial for induction of group 2 innate lymphoid cells and clearance of helminth infections. *Immunity* 46:863–874. <https://doi.org/10.1016/j.immuni.2017.04.017>.
 30. Rodbell M. 1964. Localization of lipoprotein lipase in fat cells of rat adipose tissue. *J Biol Chem* 239:753–755.
 31. Vasina V, Giannone F, Domenicali M, Latorre R, Berzigotti A, Caraceni P, Zoli M, De Ponti F, Bernardi M. 2012. Portal hypertension and liver cirrhosis in rats: effect of the β 3-adrenoceptor agonist SR58611A. *Br J Pharmacol* 167:1137–1147. <https://doi.org/10.1111/j.1476-5381.2012.02074.x>.
 32. Atarashi K, Tanoue T, Ando M, Kamada N, Nagano Y, Narushima S, Suda W, Imaoka A, Setoyama H, Nagamori T, Ishikawa E, Shima T, Hara T, Kado S, Jinnohara T, Ohno H, Kondo T, Toyooka K, Watanabe E, Yokoyama S-i, Tokoro S, Mori H, Noguchi Y, Morita H, Ivanov II, Sugiyama T, Nuñez G, Camp JG, Hattori M, Umesaki Y, Honda K. 2015. Th17 cell induction by adhesion of microbes to intestinal epithelial cells. *Cell* 163:367–380. <https://doi.org/10.1016/j.cell.2015.08.058>.
 33. Kozich JJ, Westcott SL, Baxter NT, Highlander SK, Schloss PD. 2013. Development of a dual-index sequencing strategy and curation pipeline for analyzing amplicon sequence data on the MiSeq Illumina sequencing platform. *Appl Environ Microbiol* 79:5112–5120. <https://doi.org/10.1128/AEM.01043-13>.
 34. Myer PR, Kim M, Freetly HC, Smith TP. 2016. Evaluation of 16S rRNA amplicon sequencing using two next-generation sequencing technologies for phylogenetic analysis of the rumen bacterial community in steers. *J Microbiol Methods* 127:132–140. <https://doi.org/10.1016/j.mimet.2016.06.004>.
 35. Linetzky Waitzberg D, Alves Pereira CC, Logullo L, Manzoni Jacintho T, Almeida D, Teixeira da Silva ML, Matos de Miranda Torrinhas RS. 2012. Microbiota benefits after inulin and partially hydrolyzed guar gum supplementation: a randomized clinical trial in constipated women. *Nutr Hosp* 27:123–129. <https://doi.org/10.1590/S0212-16112012000100014>.
 36. Hatamoto M, Kaneko T, Takimoto Y, Ito T, Miyazato N, Maki S, Yamaguchi T, Aoi T. 2017. Microbial community structure and enumeration of *Bacillus* species in activated sludge. *J Water Environ Technol* 15:233–240. <https://doi.org/10.2965/jwet.17-037>.
 37. Guillen IA, Camacho H, Tuero AD, Bacardí D, Palenzuela DO, Aguilera A, Silva JA, Estrada R, Gell O, Suárez J, Ancizar J, Brown E, Colarte AB, Castro J, Novoa LI. 2016. PCR conditions for 16S primers for analysis of microbes in the colon of rats. *J Biomol Tech* 3:105–112. <https://doi.org/10.7171/jbt.16-2703-002>.